On the Use of Synchrosqueezing Transform for Chaos and Nonlinear Dynamics Analysis in Fractional-Order Systems

M. Varanis ⓘ**, C. Oliveira** ⓘ**, M. A. Ribeiro** ⓘ**, W. B. Lenz** ⓘ**, A. M. Tusset** ⓘ**, and Jose Manoel Balthazar** ⓘ

Abstract In this paper, the behavior of an electromechanical device for power production is investigated. The device consists of a motor containing an unbalanced mass, which has been coupled with a system containing piezoelectric material that produces an electric current. Thus, the average power produced in the piezoelectric material subjected to the vibrations of the motor and the fractional dynamics of the system will be analyzed. For this analysis, the parameter of the fractional derivative operator and the parameter F for controlling the system are observed. Bifurcation diagrams and time–frequency analysis method based on synchrosqueezing transform are used, and the range of the fractional derivative operator parameter near 1, which modifies the dynamics of the system, is also determined.

Keywords Fractional calculus · Nonlinear dynamics · Synchrosqueezing transform

1 Introduction

With the technological advances in recent years, the great demand for energy consumption has allowed researchers to discover mechanisms that produce energy in a clean and renewable way. Thus, many works on these mechanisms have been explored. Examples of these works are those in [1–3] that explore high-degree-of-freedom mechanisms that convert mechanical energy from applied external forces into electrical energy.

Several works such as [3, 4] explore the dynamics of mechanisms for energy production. However, they propose control designs to suppress the chaotic motions.

M. Varanis (✉) · C. Oliveira
Faculdade de Engenharia, Universidade Federal da Grande Dourados, Dourados, MS, Brazil
e-mail: marcusvaranis@ufgd.edu.br

M. A. Ribeiro · W. B. Lenz · A. M. Tusset · J. M. Balthazar
Universidade Tecnológica Federal Do Paraná-Campus Ponta Grossa, Ponta Grossa, Brazil

J. M. Balthazar
Faculty of Mechanical Engineering of Bauru, São Paulo State University, Bauru, SP, Brazil

Many fractional derivative operators are used to analyze the behavior of electromechanical structures, an example is the flexibility behavior of microbeams in MEMS systems. Examples of fractional derivative operators applied for dynamic analysis are Riemann–Liouville and Grunwald Letinikov [5, 6].

In recent years, new techniques for time–frequency analysis have been proposed, one emerging technique is the synchrosqueezed transform. Known limitations, such as tradeoffs between time and frequency resolution, can be overcome by alternative techniques that extract instantaneous modal components, as presented in the synchrosqueezed transform. EMD decomposition of a signal into components that are well separated in the time–frequency plane, allowing reconstruction of these components [7]. In particular the work presented in [8], provides an overview of time–frequency reconsignment and synchronization techniques used in multicomponent signals, covering the theoretical background and applications, furthermore it tries to explain how synchrosqueezing can be seen as a special case of mode enable reconsignment reconstruction. Methods based on synchrosqueezing transform are actually an extension of CWT that incorporates elements of empirical mode decomposition and frequency reassignment techniques. This new tool produces a better-defined time–frequency representation, allowing the identification of instantaneous frequencies to highlight individual components.

Synchrosqueezing Wavelet Transform (SWT) is a time–frequency analysis method [8]. The anti-noise capability and time–frequency resolution of SWT are improved based on the wavelet transform (CWT). SWT maintains the advantages of EMD and CWT. SWT is adaptive like EMD and does not depend on the original wavelet; the mode mixing problem is significantly improved. Classical time–frequency analysis methods have been widely used in nonlinear dynamics and chaos applications [5, 7, 9–12], currently a series of applications based on synchrosqueezing have been proposed [13–17].

Therefore, will be made a fractional dynamics analysis of the model proposed by [18, 19] considering Caputo's fractional derivative operator. However, with a coupled piezoelectric in the system for the average power output and the exploration of the proposed fractional mathematical model numerically.

2 Mathematical Background

2.1 Mathematical Model

The mathematical model is based on the one proposed by [20] and the Fig. 1 shows the mechanism for application the Caputo Operator derivative.

The Eq (1) describe the motor movement and its vertical displacement of the mass, thus:

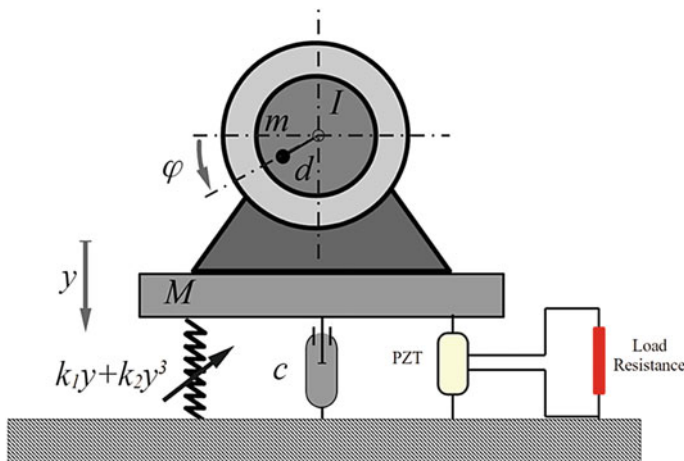$$\ddot{x}(M + m) + c\dot{x} - md\big(\ddot{\phi}sin(\phi) + \dot{\phi}^2cos(\phi)\big) + k_1x + k_2x^3$$

Fig. 1 Scheme of the structure with piezoceramic material coupled

$$+ \theta(1 + \theta_n|x|)q = (M + m)g$$
$$\ddot{\phi}(J + md^2) - md\ddot{x}\sin(\phi) + mgd\sin(\phi) = \Gamma(\dot{\phi}) \tag{1}$$

$$\rho\dot{q} - \theta(1 + \theta_n|y|)q + q = 0$$

where M mass is connected to a fixed basement by a non-linear spring and a linear viscous damper (damping coefficient c). The nonlinear spring stiffness is given by $k_1x + k_2x^3$, where x denotes the structure displacement with respect to some equilibrium position in the absolute reference frame. The motion of the structure is due to an in-board non-ideal motor driving an unbalanced rotor. Denoted by ϕ the angular displacement of the rotor unbalance, and model it as a particle of mass m and radial distance d from the rotating axis. The moment of inertia of the rotating part is J. For the resonant case the structure has an influence on the motor input or output. The forcing function is dependent of the system it acts on, and the source is of non-ideal type. And q is electrical current and θ is the linear and θ_n the nonlinear part.

Considering the following change in variables:

$$p = \frac{\omega}{\Omega}, \; \omega^2 = \frac{k_1}{M+m}, \; \gamma = \frac{k_3}{(M+m)\Omega^6}, \; \zeta = \frac{c}{(M+m)\Omega}, \; \mu = \frac{md\Omega^2}{(M+m)g}, \; \eta = \frac{gmd}{(I+md^2)\Omega^2},$$
$$F = \frac{M_0}{(I+d^2m)\Omega^2}, \; \Gamma(\dot{\phi}) = M_0\left(1 - \frac{\dot{\phi}}{\Omega}\right), \; x \rightarrow y = \frac{\Omega^2}{g}x \text{ and } t \rightarrow \tau = \Omega t.$$

Therefore, we rewrite Eq. (1):

$$\ddot{y} + \zeta\dot{y} - p^2y + \gamma y^3 = 1 + \mu\left(\ddot{\phi}\sin(\phi) + \dot{\phi}^2\cos(\phi)\right) - \theta(1 + \theta_n|y|)q$$
$$\ddot{\phi} = \eta\ddot{y}\sin(\phi) - \eta\sin(\phi) + F\left(1 - \dot{\phi}\right) \tag{2}$$

$$\dot{q} = \frac{1}{\rho}[\theta(1 + \theta_n|y|)q - q]$$

In this way, considering $y = x_1$, $\dot{y} = x_2$, $\phi = x_3$, $\dot{\phi} = x_4$ and $q = x_5$, the system of first order differential equations is obtained:

$$\dot{x}_1 = x_2$$
$$\dot{x}_2 = \frac{1}{1 - \mu\eta sin^2(y_3)}(-\zeta y_2 - py_1 - \gamma y_1^3 + 1 + \mu \sin(y_3))$$
$$(\mu y_4^2 cos(y_3) - \eta sin(y_3) + F(1 - y_4)) - \theta(1 + \theta_n|x_1|)x_5) \qquad (3)$$

$$\dot{x}_3 = x_4$$
$$\dot{x}_4 = \frac{\eta sin(y_3)}{1 - \mu\eta sin^2(y_3)}(-\zeta y_2 - py_1 - \gamma y_1^3 + 1 + \mu y_4^2 cos(y_3)$$
$$+ \mu sin(y_3)(-\eta sin(y_3) + F(1 - y_4))) - \eta sin(y_3) + F(1 - y_4)$$
$$\dot{x}_5 = \frac{1}{\rho}[\theta(1 + \theta_n|x_1|)x_5 - x_5]$$

The Caputo operator is defined as follows [11–18]:

$$_a^C D^q f(t) = \frac{1}{\Gamma(q - n)} \int_a^t \frac{f^{(n)}(\tau)d\tau}{(t - \tau)^{q+1-n}} \qquad (4)$$

where $n - 1 < q < n$, in our considerations n $= 1$, thus, $0 < q < 1$ and $\Gamma(.)$ is defined as the gamma function. Therefore, rewrite the System of Differential Equations considering the Caputo operator for analyses:

$$_a^C D^q x_1 = x_2$$
$$_a^C D^q x_2 = \frac{1}{1 - \mu\eta sin^2(y_3)}(-\zeta y_2 - py_1 - \gamma y_1^3 + 1$$
$$+ \mu \sin(y_3)(\mu y_4^2 cos(y_3) - \eta sin(y_3) + F(1 - y_4)))$$
$$- \theta(1 + \theta_n|x_1|)x_5)$$
$$_a^C D^q x_3 = x_4 \qquad (5)$$

$$_a^C D^q x_3 = \frac{\eta sin(y_3)}{1 - \mu\eta sin^2(y_3)}(-\zeta y_2 - py_1 - \gamma y_1^3 + 1$$
$$+ \mu y_4^2 cos(y_3) + \mu sin(y_3)(-\eta sin(y_3) + F(1 - y_4)))$$
$$- \eta sin(y_3) + F(1 - y_4)$$
$$_a^C D^q x_5 = \frac{1}{\rho}[\theta(1 + \theta_n|x_1|)x_5 - x_5]$$

2.2 Synchrosqueezed Transform

STFT and CWT are the main approaches to simultaneously decompose a signal into time and frequency components. Known limitations, such as tradeoffs between time and frequency resolution, can be overcome by alternative techniques that extract instantaneous modal components. EMD aims to decompose a signal into components that are well separated in the time–frequency plane, allowing reconstruction of these components. On the other hand, a recently proposed method called the synchrosqueezing transform (SST) is an extension of the wavelet transform that incorporates elements of empirical mode decomposition and frequency reassignment techniques. This new tool produces a well-defined time–frequency representation, allowing the identification of instantaneous frequencies in non-stationary signals to highlight individual components.

SST was initially proposed in the wavelet case [8] and then later extended to the STFT case [7, 8]. In fact, it corresponds to a nonlinear operator that bounces the time–frequency representation of a signal, combining the localization and scattering properties of the Reassignment Methods with the invertibility property of linear time–frequency representations.

2.3 Synchrosqueezing Wavelet Transform

The Synchrosqueezing Wavelet Transform calculation consists of three steps. The first step is to calculate the CWT. In the second step, a preliminary frequency ω (a, b) is obtained from the oscillatory behavior of W_x (a, b) at a, so that:

$$\omega(a, b) = -i(W_x(a, b))^{-1} \frac{\partial}{\partial a} W_x(a, b) \qquad (6)$$

In the third step the transformation from the time scale plane to the time–frequency plane is performed. Each value of W_x (a, b) is assigned again to (a, ωl). Where ωl denotes the frequency that is closest to the preliminary frequency of the original (discrete) point ω (a, b). This operation is presented in Eq. (7):

$$T(a, \omega_1) = (\Delta\omega)^{-1} \sum_{b_k:|\omega(a,b_k)-\omega l|\leq\Delta\omega/2} W x(a, b_k) b_k^{-3/2} \Delta b \qquad (7)$$

In Eq. (7) $\Delta\omega$ denotes the width of each frequency b in $\Delta\omega = \omega\_l - \omega\_(l-1)$ and equivalently for Δb. SWT can obtain a high-resolution time–frequency spectrum by compressing (reassigning) the CWT result. However, when the amplitude of the high-frequency components of a signal is low, it is difficult to identify the components in the CWT spectrum or the SST spectrum that is based on the CWT result. In contrast to CWT, the SWT transform is able to more efficiently display the high frequency, low amplitude components of a signal and perform a lossless inverse transformation.

Originally proposed in the wavelet case, the SST has been similarly extended to the STFT context, known as the Fourier-based synchrosqueezing transform (FSST). A long study and in-depth formulation on STFT, CWT and FSST can be seen in [21–24].

3 Numerical Results and Discussion

For the numerical analysis, using the following initial conditions x0 = [0,0,0,0] and for analysis corresponds to q = [0.978- 1]. Thus, we analyzed the behavior of fractional dynamics for values close to 1, which we could observe some chaotic windows in the system. The parameters is: $\eta = 0.05$, $\mu = 8.737$, $p = 1.0$, $\gamma = 9.0$, $\theta = 0.1$, $\theta_n = 0.5$, $\zeta = 0.2$, $\theta = 0.1$ and $\theta_n = 0.5$ [20].

The numerical method for solving the Eq. (5) is composed of the initial value problem and the variational system and Adams–Bashforth-Moulton scheme for fractional differential equations [20–24], with a h = 0.001 and a time of 10^5 [s] considering 40% of total time with transient time. Utiliza-se métodos de análise tempo-frequência para caracterizar a dinâmica caótica do sistema, ente eles CWT e métodos baseados em synchrosqueezing transform, em especial, Fourier-based synchrosqueezing transform e synchrosqueezing wavelet transform [4, 9, 14].

Therefore, Fig. 2 shows the behavior of the bifurcation diagrams of the systems, and considering $F = [23., 46.6, 70]$, we can observe the emergence of chaotic windows with the variation of the parameter of the fractional derivative.

Figure 2a observes the chaotic windows at q = [0.9790:9793], [0.9816, 0.9822], [0.9871, 0.9873], [0.9887, 0.9936] and q = [0.995; 1.0] with parameter F = 23.3. According to [9] for F = 23.3 and q = 1, which results in the conventional derivative operator, so the system exhibits chaotic regime. This happens for q = 1 at F = 46.6 and 70 has a chaotic behavior which corroborates the data collected by [9], where for systems with the entire derivative operator the system is in a chaotic regime. In Fig. 2b with F = 46.6 has the following chaotic windows q = [0.978, 0.9783], q = [0.9875, 0.9876], q = [0.9937, 0.9941], q = [0.9946, 0.9952] and q = [0.9976;1] and in Fig. 2c q = [0.978; 0.9737], q = [0.9871; 0.9875], q = [0.9919; 0.992], q = [0.9921; 0.9928], q = [0.9942; 0.996] and q = [0.9983; 1]. In Fig. 2c with F = 70 has the following chaotic windows q = [0.978, 0.9783], q = [0.9875, 0.9876], q = [0.9937, 0.9941], q = [0.9946, 0.9952] and q = [0.9976;1] and in Fig. 3c q = [0.978; 0.9737], q = [0.9871; 0.9875], q = [0.9919; 0.992], q = [0.9921; 0.9928], q = [0.9942; 0.996] and q = [0.9983; 1]. Thus, through the bifurcation diagrams we can observe the correspondence of the intervals in which the chaotic behavior of the subintervals contained in the interval q = [0.978, 1.0].

Next in Fig. 3 is presented the time–frequency analysis of the system for F = 23 and q = 0.98. In Fig. 3a the phase diagram is presented. Already in Fig. 3b is presented the response of the system in the frequency domain to CWT and it is possible to identify the periodicity of the system, as well as to identify the dominant frequency and the multiple frequencies, typical of systems with cubic nonlinearity,
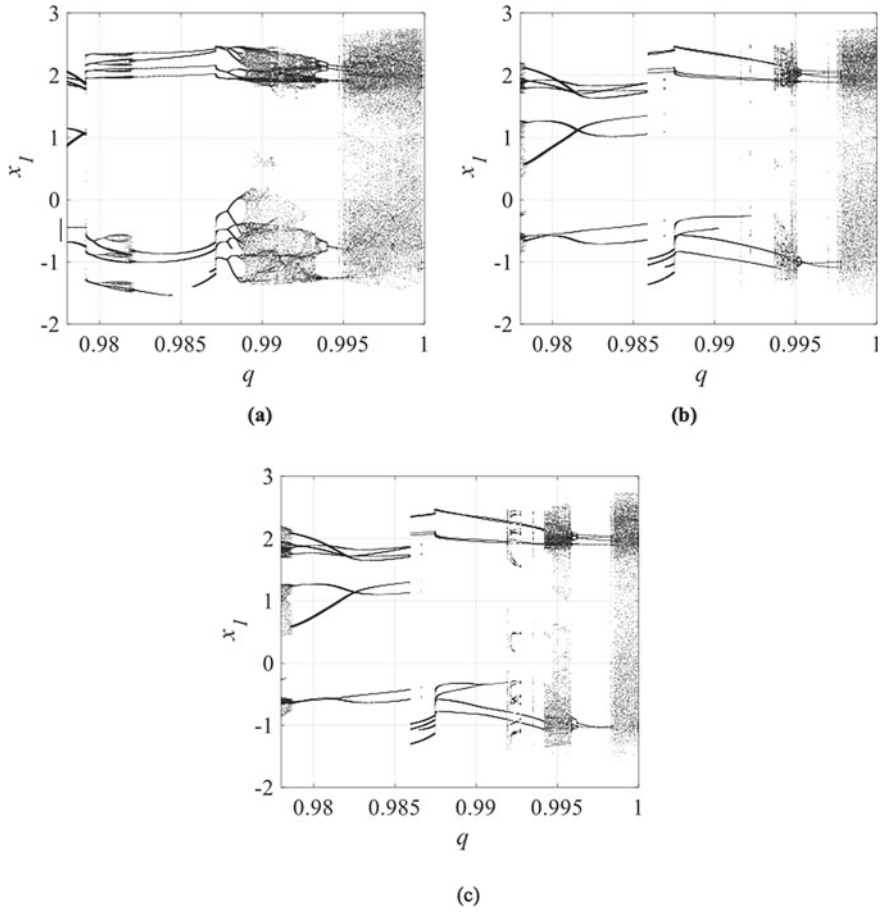
Fig. 2 Bifurcation diagram for $q = [0.978, 1.0]$: **a** $F = 23.3$, **b** $F = 46.6$ and **c** $F = 70$
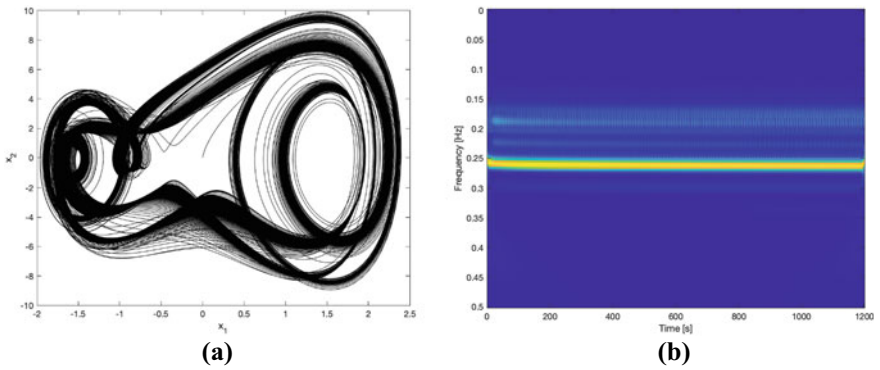

Fig. 3 $F = 23$, $q = 0,98$: **a** Phase diagram, **b** CWT

but there is still an energy dispersion in the time–frequency plane, which does not make the analysis suitable for application. Meyer's wavelet [4] was used in the CWT analysis.

In Fig. 4 the time–frequency analysis of the system (F $=$ 23 and q $=$ 0.98) using synchrosqueezing transform based methods is presented. In Fig. 4a the system response is analyzed using the Fourier-based synchrosqueezing transform (FSST), it is possible to characterize the periodicity of the system, as well as identify the dominant frequency and the multiple frequencies, but the method presents low resolution in the time–frequency plane. In Fig. 4b is presented the system response in the frequency domain using SWT, in this case it is possible, quite clearly, to identify the periodicity of the system, as well as to identify the dominant frequency and the multiple frequencies and notice that the energy dispersion in the time–frequency plane is very small.
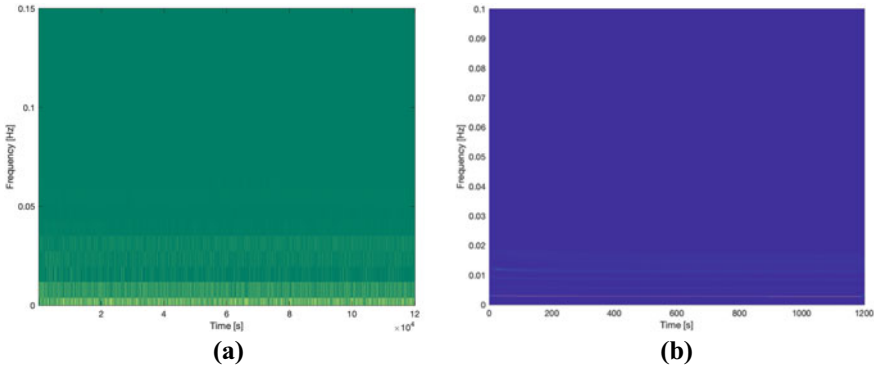

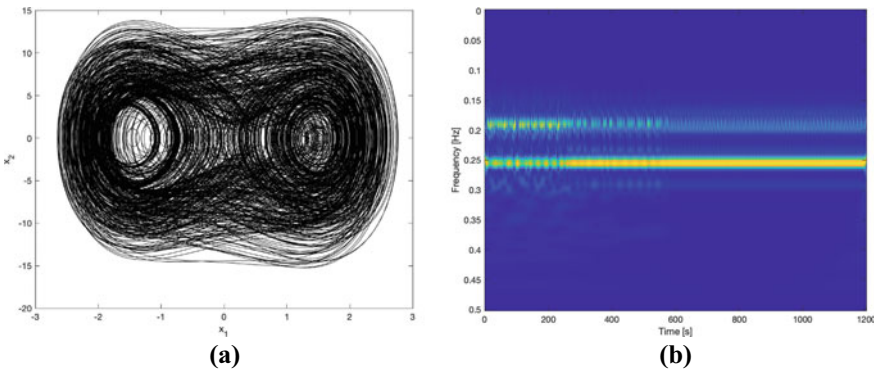**Fig. 4** F $=$ 23, q $=$ 0,98: **a** S-SFT, **b** SWT

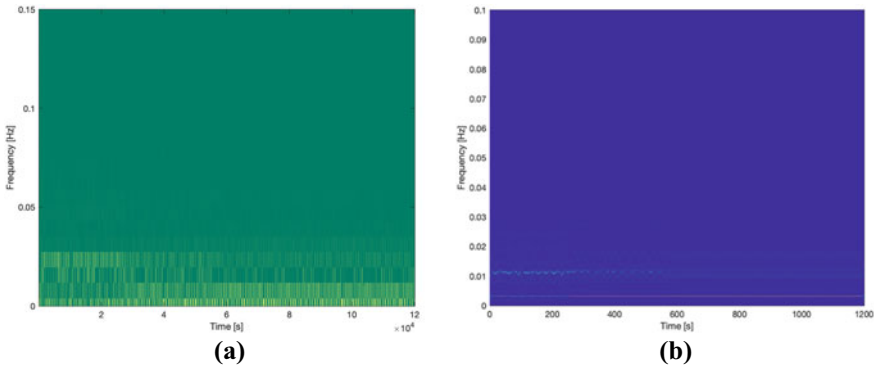**Fig. 5** F $=$ 23, q $=$ 1: **a** Phase diagram, **b** CWT

Fig. 6 F = 23, q = 1: **a** S-SFT, **b** SWT

In Fig. 5 is presented the time–frequency analysis of the system for F = 23 and q = 1, for these parameters the system exhibits chaotic dynamics, as shown in the bifurcation diagram (Fig. 2a). In Fig. 5a the phase diagram of the system is presented. In Fig. 5b the response of the system in the frequency domain to CWT is presented, it is still possible to identify the dominant frequency, but the response presents a large scattering and abrupt change in the frequency spectrum, typical characteristic of chaotic systems [4, 14].

Figure 6 presents the time–frequency analysis of the system (F = 23 and q = 1) using synchrosqueezing transform based methods. The system response is analyzed using FSST (Fig. 6a), it is noted that there was large scattering and abrupt change in the frequency spectrum, but due to low resolution and large energy dispersion in the time–frequency plane, it is not possible to characterize the chaotic dynamics of the system. In Fig. 6b is presented the response of the system in the frequency domain using SWT, in this case it is possible to identify the dominant frequency and the response presents a large scattering and abrupt change in the frequency spectrum, but the energy dispersion in the time–frequency plane is very small, which makes the technique quite accurate and appropriate.

Next in Fig. 7 is presented the time–frequency analysis of the system for F = 46.6 and q = 0.985. Again, the phase space is presented (Fig. 7a) and the CWT response of the system in the frequency domain (Fig. 7b). The response via CWT allows the periodicity of the system to be identified, as well as easily identifying the dominant frequency and multiple frequencies.

In Fig. 8 the time–frequency analysis of the system (F = 46.6 and q = 0.985) using synchrosqueezing transform based methods is presented. The response of the system using FSST is presented in Fig. 8a, the large energy dispersion and low resolution in the time–frequency plane do not allow to characterize the periodicity of the system, also the dominant frequency and multiple frequencies cannot be identified with the necessary clarity. In Fig. 8b the response of the system (F = 23 and q = 0.98) in the frequency domain using SWT is presented, in this case it is possible to identify the periodicity of the system, as well as to identify the dominant frequency and the multiple frequencies.
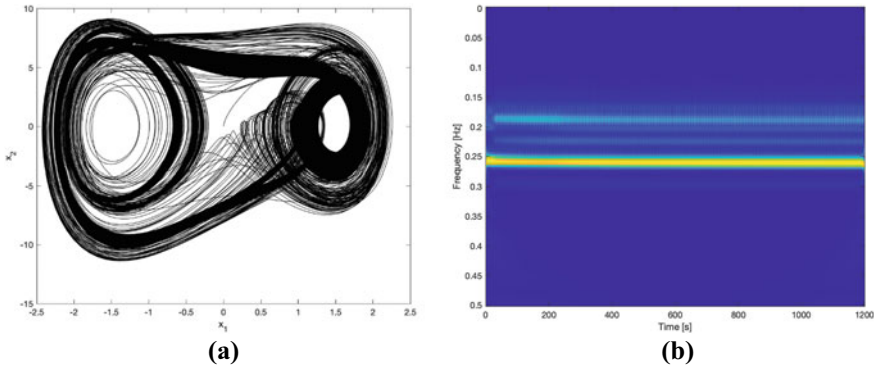
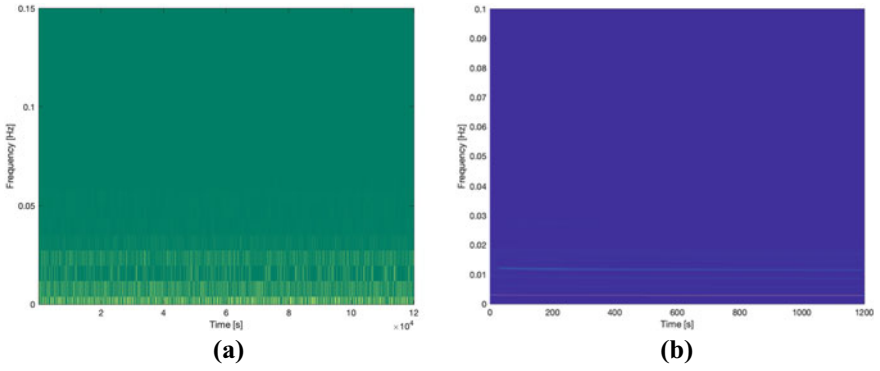**Fig. 7** F = 46.6, q = 0.985: **a** Phase diagram, **b** CWT

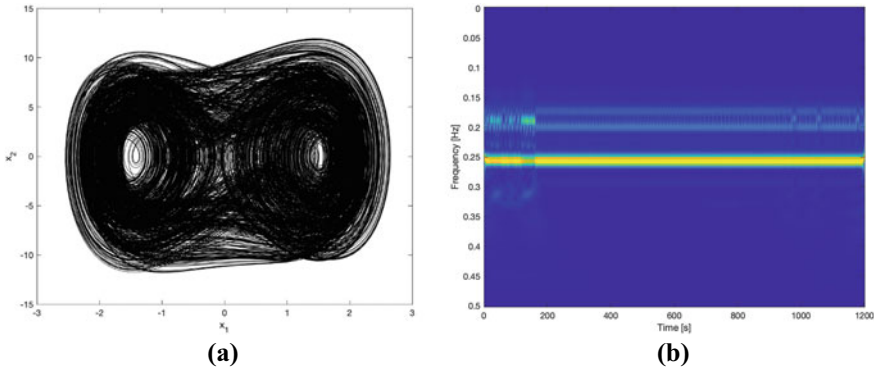**Fig. 8** F = 46.6, q = 0.985: **a** S-SFT, **b** SWT

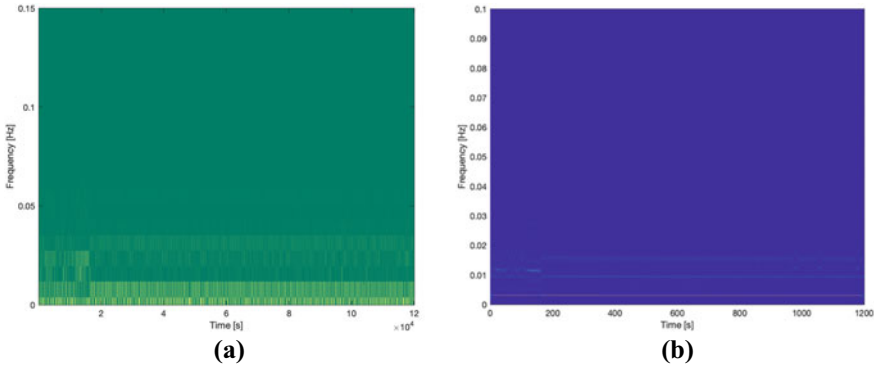**Fig. 9** F = 46.6, q = 1: **a** Phase diagram, **b** CWT

Fig. 10 F = 46,6, q = 0,995: **a** FSST, **b** SWT

Figure 9 presents the time–frequency analysis of the system for F = 46.6 and q = 1, for these parameters the system exhibits chaotic dynamics as presented in the bifurcation diagram (Fig. 2b). In Fig. 9a the phase diagram of the system is presented. In Fig. 9b is presented the response of the system in the frequency domain to CWT, one can clearly identify the dominant frequency, but the response presents a large scattering and abrupt change at the beginning of the frequency spectrum, indicating chaos in the system.

In Fig. 10a the response of the system using FSST is presented, it can be seen that there was a large scattering and abrupt change in the frequency spectrum, but due to low resolution and large energy dispersion in the time–frequency plane, it is not possible to clearly characterize the chaotic dynamics of the system. The SWT analysis (Fig. 10b) shows that it is possible to identify the dominant frequency and a large scattering and abrupt change in the frequency spectrum at the beginning of the response, again the low energy dispersion allows the characterization of the chaotic dynamics of the system.

Next in Fig. 11 is presented the time–frequency analysis of the system for F = 70 and q = 0.995. Again, the phase space is presented (Fig. 11a) and the system response in the frequency domain to CWT (Fig. 11b). The response via CWT allows, as in the previous cases, the periodicity of the system to be identified, as well as easily identifying the dominant frequency and multiple frequencies. The same occurs with analysis via FSST (Fig. 12c) and SWT (Fig. 12d).

Finally, Fig. 13 presents the time–frequency analysis of the system for F = 70 and q = 0.999. The phase space (Fig. 13a) shows the rich dynamics of the system and the response of the system in the frequency domain to CWT (Fig. 13b) characterizing the chaotic dynamics in the system. In (Fig. 14a) shows the response of the system with the use of FSST, it is noted that there was large scattering and abrupt change in the frequency spectrum, as in previous cases, it is not possible to clearly characterize the chaotic dynamics of the system. The analysis using SWT (Fig. 14b), shows that it is possible to identify the dominant frequency and a large scattering and abrupt change in the frequency spectrum, in order to characterize the chaotic dynamics of the system.
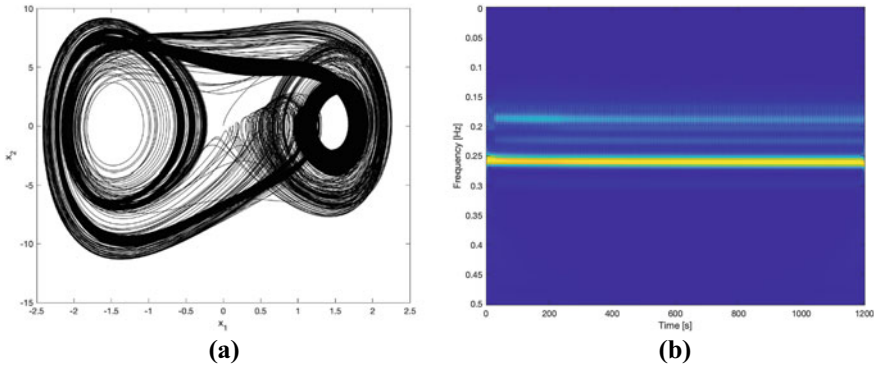
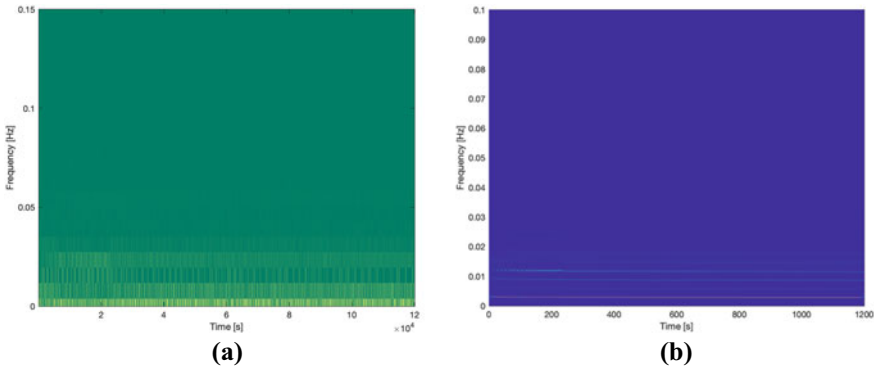**Fig. 11** F = 70, q = 0,995: **a** Phase diagram, **b** STFT
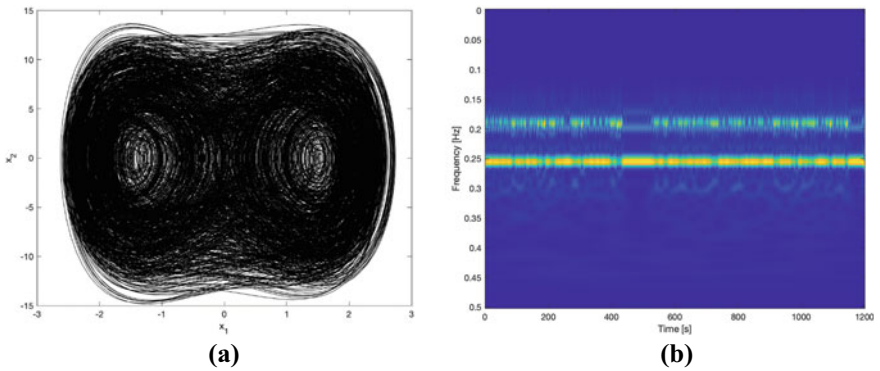

Fig. 12 F = 70, q = 0.985: **a** S-SFT, **b** SWT

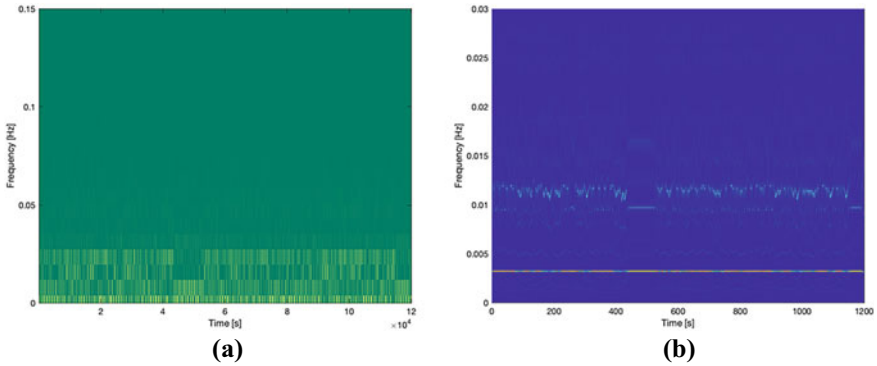**Fig. 13** F = 70, q = 0.999: **a** Phase diagram, **b** CWT

Fig. 14 F = 70, q = 0,999: **a** S-SFT, **b** SWT

4 Conclusion

The fractional model for energy harvesting presented in the interval q = [0.958, 1] a chaotic behavior for the structure with Caputo's fractional derivative operator. Thus, bifurcation diagrams and synchrosqueezing-based transform were used to analyze the location of these windows, for a set of F parameters and characterize the chaotic dynamics of the system. Therefore, it was determined for values close to q = 1, regions that exhibited chaotic and periodic behavior. These regions are confirmed in the bifurcation diagrams, CWT and SWT. The analysis of the fractional dynamics of the system not only corroborates the generalization of the mathematical model in a numerical form, but also in the behavior with the Caputo fractional derivative operator. CWT-based techniques show good resolution in the time–frequency plane, but CWT still overshadows other components when there are high concentrations of energy at some signal frequency. Applications of wavelet transform-based techniques to nonlinear systems have demonstrated the ability of this technique to monitor signal frequency variations and detect short-term transients with excellent time–frequency localization, far exceeding the limitations presented by Fourier transform-based techniques such as STFT.

Finally, the results obtained using the synchrosqueezed wavelet transform were excellent, showing very good time–frequency resolution and minimal energy dispersion, proving adequate to characterize the chaotic dynamics of the system.

References

1. Ribeiro, M. A., Balthazar, J. M., Lenz, W. B., Rocha, R. T., Tusset, A. M.: Numerical exploratory analysis of dynamics and control of an atomic force microscopy in tapping mode with fractional order. Shock and Vib. 2020 (2020)
2. Tusset, A. M., Balthazar, J. M., Ribeiro, M. A., Lenz, W. B., Rocha, R. T.: Chaos control of an atomic force microscopy model in fractional-order. Eur Phys J Spec Top 1–12 (2021)
3. Tusset, A.M., Ribeiro, M.A., Lenz, W.B., Rocha, R.T., Balthazar, J.M.: Time delayed feedback control applied in an atomic force microscopy (AFM) model in fractional-order. J. Vib. Eng. Technol. **8**(2), 327–335 (2020)
4. Varanis, M. V., Tusset, A. M., Balthazar, J. M., Litak, G., Oliveira, C., Rocha, R. T., Piccirillo, V.: Dynamics and control of periodic and non-periodic behavior of Duffing vibrating system with fractional damping and excited by a non-ideal motor. J. Frankl. Inst. **357**(4), 2067–2082 (2020)
5. Iliuk, I., Balthazar, J.M., Tusset, A.M., Piqueira, J.R.C., de Pontes, B.R., Felix, J.L.P., et al.: A non-ideal portal frame energy harvester controlled using a pendulum. Eur. Phys. J. Spec. Top. **222**, 1575–1586 (2013)
6. Iliuk, I., Balthazar, J.M., Tusset, A.M., Piqueira, J.R., de Pontes, B.R., Felix, J.L., et al.: A non-ideal portal frame energy harvester controlled using a pendulum. Eur. Phys. J. Spec. Top. **222**(7), 1575–1586 (2013)
7. Varanis, M., Silva, A. L., Balthazar, J. M., Pederiva, R.: A tutorial review on time-frequency analysis of non-stationary vibration signals with nonlinear dynamics applications. Braz. J. Phys. 1–19 (2021)
8. Daubechies, I., Lu, J., Wu, H.T.: Synchrosqueezed wavelet transforms: an empirical mode decomposition-like tool. Appl. Comput. Harmon. Anal. **30**(2), 243–261 (2011)
9. Varanis, M., Balthazar, J.M., Silva, A., Mereles, A.G., Pederiva, R.: Remarks on the sommerfeld effect characterization in the wavelet domain. J. Vib. Control **25**(1), 98–108 (2019)
10. Li, Y., Sun, R., Yin, K., Xu, Y., Chai, B., Xiao, L.: Forecasting of landslide displacements using a chaos theory based wavelet analysis-Volterra filter model. Sci. Rep. **9**(1), 1–19 (2019)
11. Mao, J., Zhang, X., Li, J.: Wind power forecasting based on chaos and wavelet packet theory. In 2018 13th IEEE Conference on Industrial Electronics and Applications (ICIEA) (pp. 1604–1608). IEEE (2018)
12. Cattani, C.: A review on harmonic wavelets and their fractional extension. J. Adv. Eng. Comput **2**(4), 224–238 (2018)
13. Hu, J., Liu, B., Yu, M.: A novel method of realizing stochastic chaotic secure communication by synchrosqueezed wavelet transform: the finite-time case. IEEE Access (2021)
14. Varanis, M., Norenberg, J.P.C., Rocha, R.T., Oliveira, C., Balthazar, J.M., Tusset, A.M.: A comparison of time-frequency methods for nonlinear dynamics and chaos analysis in an energy harvesting model. Braz. J. Phys. **50**(3), 235–244 (2020)
15. He, K., Li, Q., Yang, Q.: Characteristic analysis of welding crack acoustic emission signals using synchrosqueezed wavelet transform. J. Test. Eval. **46**(6), 2679–2691 (2018)
16. Hasan, F.S.: Chaotic signals denoising using empirical mode decomposition inspired by multivariate denoising. Int. J. Electr. Comput. Eng. **10**, 1352–1358 (2020)
17. Alugongo, A. A. (2021). Experimental study of the impact of the fluid forces on disturbances induced by the rotor-stator rubbing (Part II). In 2021 IEEE 12th International Conference on Mechanical and Intelligent Manufacturing Technologies (ICMIMT), pp. 133–138. IEEE (2021)
18. Iliuk, I., Brasil, R.M.L.R.F., Balthazar, J.M., Tusset, A.M., Piccirillo, V., Piqueira, J.R.C.: Potential application in energy harvesting of intermodal energy exchange in a frame: FEM analysis. Int. J. Struct. Stab. Dyn. **14**(8), 1440027 (2014)
19. Iliuk, I., Balthazar, J.M., Tusset, A.M., Piqueira, J.R., de Pontes, B.R., Felix, J.L., et al.: Application of passive control to energy harvester efficiency using a nonideal portal frame structural support system. J. Intell. Mater. Syst. Struct. **25**(4), 417–429 (2014)

20. Gonçalves, A., Ribeiro, M. A., Gunha, J. V., Somer, A., Zanuto, V. S., Astrath, N. G., Novatski, A.: A generalized Drude–Lorentz model for refractive index behavior of tellurite glasses. J. Mater. Sci. Mater. Electron. **30**(18), 16949–16955 (2019)
21. Flandrin, P., Auger, F., Chassande-Mottin, E. (2018). Time-frequency reassignment: from principles to algorithms. In Applications in time-frequency signal processing, pp. 179–204. CRC Press
22. Flandrin, P.: Explorations in Time-Frequency Analysis. Cambridge University Press (2018)
23. Fourer, D., Auger, F., Czarnecki, K., Meignen, S., Flandrin, P.: Chirp rate and instantaneous frequency estimation: application to recursive vertical synchrosqueezing. IEEE Signal Process. Lett. **24**(11), 1724–1728 (2017)
24. Addison, P.S.: The illustrated wavelet transform handbook: introductory theory and applications in science, engineering, medicine and finance. CRC Press (2017)